Since January 2020 Elsevier has created a COVID-19 resource centre with free information in English and Mandarin on the novel coronavirus COVID-19. The COVID-19 resource centre is hosted on Elsevier Connect, the company's public news and information website.

Machine learning and semi-targeted lipidomics identify distinct serum lipid signatures in hospitalized COVID-19-positive and COVID-19-negative patients

Helena Castañé, Simona Iftimie, Gerard Baiges-Gaya, Elisabet Rodríguez-Tomàs, Andrea Jiménez-Franco, Ana Felisa López-Azcona, Pedro Garrido, Antoni Castro, Jordi Camps, Jorge Joven

PII: S0026-0495(22)00075-0

DOI: https://doi.org/10.1016/j.metabol.2022.155197

Reference: YMETA 155197

To appear in: *Metabolism*

Received date: 10 December 2021

Accepted date: 28 March 2022

Please cite this article as: H. Castañé, S. Iftimie, G. Baiges-Gaya, et al., Machine learning and semi-targeted lipidomics identify distinct serum lipid signatures in hospitalized COVID-19-positive and COVID-19-negative patients, *Metabolism* (2021), https://doi.org/10.1016/j.metabol.2022.155197

Machine learning and semi-targeted lipidomics identify distinct serum lipid signatures in hospitalized COVID-19-positive and COVID-19-negative patients

Helena Castañé [a,1], Simona Iftimie [b,1], Gerard Baiges-Gaya [a], Elisabet Rodríguez-Tomàs [a], Andrea Jiménez-Franco [a], Ana Felisa López-Azcona [b], Pedro Garrido [c], Antoni Castro [b,] Jordi Camps [a,]*, Jorge Joven [a]

[a] *Unitat de Recerca Biomèdica, Hospital Universitari de Sant Joan, Institut d'Investigació Sanitària Pere Virgili, Universitat Rovira i Virgili, Reus, Spain*

[b] *Department of Internal Medicine, Hospital Universitari de Sant Joan, Institut d'Investigació Sanitària Pere Virgili, Universitat Rovira i Virgili, Reus, Spain*

[c] *Intensive Care Unit, Hospital Universitari de Sant Joan. Institut d'Investigació Sanitària Pere Virgili, Universitat Rovira i Virgili, Reus, Spain.*

* *Corresponding author at:* Unitat de Recerca Biomèdica, Hospital Universitari de Sant Joan, C. Sant Joan s/n, 43201 Reus, Spain. Phone: +34977310300. Fax: +34977312569. *E-mail address:* (jorge.camps@salutsantjoan.cat) (J. Camps).

[1] Helena Castañé and Simona Iftimie contributed equally to this manuscript.

Short title: Serum lipidomics in COVID-19

Keywords: artificial intelligence; COVID-19; lipid metabolism; lipidomics; machine learning

ABSTRACT

Background: Lipids are involved in the interaction between viral infection and the host metabolic and immunological responses. Several studies comparing the lipidome of COVID-19-positive hospitalized patients *vs.* healthy subjects have already been reported. It is largely unknown, however, whether these differences are specific to this disease. The present study compared the lipidomic signature of hospitalized COVID-19-positive patients with that of healthy subjects, as well as with COVID-19-negative patients hospitalized for other infectious/inflammatory diseases.

Methods: We analyzed the lipidomic signature of 126 COVID-19-positive patients, 45 COVID-19-negative patients hospitalized with other infectious/inflammatory diseases and 50 healthy volunteers. A semi-targeted lipidomics analysis was performed using liquid chromatography coupled to mass spectrometry. Two-hundred and eighty-three lipid species were identified and quantified. Results were interpreted by machine learning tools.

Results: We identified acylcarnitines, lysophosphatidylethanolamines, arachidonic acid and oxylipins as the most altered species in COVID-19-positive patients compared to healthy volunteers. However, we found similar alterations in COVID-19-negative patients who had other causes of inflammation. Conversely, lysophosphatidylcholine 22:6-sn2, phosphatidylcholine 36:1 and secondary bile acids were the parameters that had the greatest capacity to discriminate between COVID-19-positive and COVID-19-negative patients.

Conclusion: This study shows that COVID-19 infection shares many lipid alterations with other infectious/inflammatory diseases, and which differentiate them from the healthy population. The most notable alterations were observed in oxylipins, while alterations in bile acids and glycerophospholipis best distinguished between COVID-19-positive and COVID-19-negative patients. Our results highlight the value of integrating lipidomics with machine learning algorithms to explore the pathophysiology of COVID-19 and, consequently, improve clinical decision making.

1. Introduction

To date, the coronavirus disease 2019 (COVID-19) pandemic has, according to data from the WHO [1], affected 349 million people worldwide, causing 5.5 million deaths. Knowledge of the risk factors and symptoms would help curb infection and transmission rates. Developing screening tests and effective therapies have been the urgent issues that most studies have addressed i.e. most studies have been directed toward describing the clinical and epidemiological characteristics of COVID-19 [2-6] or have investigated the "cytokine storm" associated with the infection, with the urgent objective of combating the pandemic in the short term [7,8] while bearing in mind that COVID-19 will not be eradicated easily, and that populations would need to accommodate for the infection in the future. Indeed, although vaccination campaigns are progressing effectively in financially well-established countries, infection continues to increase rapidly in many countries that have poor health infrastructures. With extensive infection and re-infection, there is potential for new variants of SARS-CoV-2 which would keep world-wide infection rates high. Hence, medium and long-term research efforts aimed at developing strategies for identifying and treating COVID-19 also remain correspondingly high. SARS-CoV-2 infection produces dramatic changes in the metabolism of the host cell, including the concentration and composition of different lipid species [9,10]. Lipids combine with thousands of metabolites and hundreds of specific pathways in support of the life-cycle of an organism [11]. As such, it is not surprising that these compounds are involved in the interplay between viral infection and the host's response [10]. Viruses are internalized into cells through protein-lipid interactions [12,13] and are externalized via lipid vesicles [14]. Interactions between viruses and the organism alter mitochondrial metabolism and the microbiota [15-17]. Further, lipids are bioactive molecules in the organism's immune system and small differences in their chemical structures can have a strong impact on the immune response [18,19]. For example, eicosanoids have signaling functions that depend on the location or orientation of a hydroxyl group in the fatty acid chain, small alterations in which result in anti- or pro-inflammatory stimuli [20]. Oxidative stress triggered by infection profoundly alters the lipid composition of the host cells and circulation. Oxidized lipids are produced via specific biosynthetic pathways and involve the direct action of free radical species on polyunsaturated fatty

acids. The resultant interference with the functions of various enzymes has significant biological consequences [21] which are difficult to quantify metabolically. Fortunately, the advent of powerful tools of metabolomics techniques in combination with bioinformatics and artificial intelligence are of considerable help in understanding the interactions between infectious processes and the metabolic responses of the host [19-23]. Studies comparing the lipidome of COVID-19-positive patients *vs.* healthy subjects have been reported, and distinctive lipid species have been identified [10]. However, there is a paucity of information regarding the specificity of these measurements, i.e. whether variations in circulating levels of the species identified are characteristic of the COVID-19 infection, or whether they can be observed in other infectious or inflammatory diseases, as well. Our study was aimed at identifying alterations in the serum lipidome of patients with COVID-19 infection, the aim being to evaluate the relationships between the alterations and the disease and. as such, to identify potential biomarkers that would help in clinical decisions in diagnosis and treatment.

2. Materials and methods

2.1. Study design and participants

We performed a retrospective *post-hoc* cohort study in 126 patients hospitalized for COVID-19 infection between March and October 2020 in the Department of Internal Medicine, or in the Intensive Care Unit (ICU) of our Institution. Inclusion criteria into the present study were: ≥18 years of age and a positive PCR result for COVID-19 obtained within 24 hours before the blood sample was drawn for the study. Exclusion criteria were: having a life expectancy ≤24 hours, impaired liver function, or pregnancy. We also analyzed samples from 45 COVID-19-negative patients hospitalized with diseases having an infectious/inflammatory component. These samples, collected in 2019, belonged to a previous prospective study in patients with urinary catheter-related infection. A detailed description of these patients has been published [24]. For the purposes of the present study, we selected a subgroup with a distribution of age and sex to match, as closely as possible, the COVID-19-positive patients. As a control group, we analyzed samples from 50 healthy volunteers who had participated in an epidemiological study, the details of which have already been

reported [25]. The subjects had no clinical or biochemical evidence of diabetes, cancer, kidney failure, liver disease, or neurological disorders. Serum samples from all participants were stored in our Biobank at –80ºC until the time of batched analyses. We recorded clinical and demographic data and calculated the McCabe score as an index of clinical prognosis [26] and the Charlson index as a way of categorizing patient comorbidities [27]. This study was approved by the *Comitè d'Ètica i Investigació en Medicaments* (Institutional Review Committee) of the *Institut d'Investigació Sanitària Pere Virgili* (Resolution CEIM 040/2018, modified on April 16, 2020).

2.2. Lipidomics analyses

A total of 283 lipid species were analyzed by semi-targeted lipidomics. This approach differs from targeted lipidomics in that it does not use a specific standard for each of the 283 lipid species analyzed but, instead, selects a small sample set of standards from each of the different lipid classes. The calibration curves so obtained were used for the quantification of their corresponding lipid species. The rest of the compounds were quantified using a standard that belongs to the same lipid class and has a similar chemical structure. In addition, labeled internal standards were used to correct the response of each detected lipid species. The standards used were the following: For acylcarnitine determination, L-carnitine, O-acetyl-L-carnitine, O-propionyl-L-carnitine, O-butyryl-L-carnitine, O-isovaleryl-L-carnitine, O-octanoyl-L-carnitine, O-myristoyl-L-carnitine, O-palmitoyl-L-carnitine, O-glutaryl-L-carnitine, O-3-hydroxyisovaleryl-L-carnitine, O-dodecanoyl-L-carnitine, O-octadecanoyl-L-carnitine, and O-3-DL-hydroxypalmitoyl-L-carnitine. Internal standards were trimethyl-D9, N-methyl-D3, N,N,N,-methyl-D9, and N-methyl-D9 (Cambridge Isotope Laboratories, Andover, MA, USA). For polar lipids determination, lipid standards were lysophosphatidylethanolamine (LPE) 16:0, lysophosphatidylcholine (LPC) 18:0, dehydroepiandrosterone 3-sulfate, cortisol, cholic acid, taurocholic acid, deoxycholic acid, arachidonic acid, and 15-hydroxyeicosatetraenoic acid (15-HETE), and the set of labeled lipid as internal standards were LPC 18:1-d7, cholic acid-d4, taurocholic acid-d5, arachidonic acid-d8, and myristic acid-d27 (Avanti Polar Lipids, Alabaster, AL, USA). Lastly, standards for the determination of non-polar lipids were LPC 18:0, phosphatidylcholine (PC) 32:0, sphingomyelin (SM) 36:1, diglyceride (DG) 36:0,

triglyceride (TG) 52:3, and cholesteryl ester (CE) 16:0, and the set of labeled lipid internal standards was the SPLASH mixture from Avanti Polar Lipids. Analytical methods have been previously reported by our research group [28,29]. Briefly, acylcarnitines and polar lipids were extracted with methanol and non-polar lipids were extracted with a mixture of tert-buthyl ether and methanol (1:2 v/v) with 0.5% acetic acid. The extracts were injected into a 1290 Infinity ultra-high-pressure liquid chromatograph (UHPLC) coupled to a 6550 quadrupole-time-of-flight mass spectrometer (QTOF) using a dual jet stream electrospray ionization (ESI) source (Agilent Technologies, Santa Clara, CA, USA). The system was equipped with a binary pump (G4220A) and an autosampler (G4226A) thermostat-controlled at 4ºC. Acylcarnitines were separated in a Kinetex 2.6 µm Polar C18, 100 Å, 150 x 2.1 mm column, (Phenomenex, Torrance, CA, USA). The mobile phase consisted of A: 99.9% water + 0.1% formic acid; B: 99.9% methanol with 0.1% formic acid, at a flow rate of 0.4 mL/min. The gradient used was as follows: 0 min, 0% B; 11 min, 100% B, 13 min, 0%B, 16.5 min, 0%B. Polar lipids were separated in an Acquity BEH C_{18} column 1.7 µm, 2.1 mm × 100 mm (Waters Corp., Milford, MA, USA). The mobile phase consisted of A: water + 0.05% formic acid; B: acetonitrile + 0.05 formic acid. The flow rate was 0.3 mL/min. The gradient used was as follows: 0 min, 2% B; 2 min, 50% B; 10 min, 98% B; from 10 to 13 min, gradient was maintained at 98% B for column cleaning; 14 min, 2% B followed by a post-run of 4 min under the same conditions for column re-conditioning. Non-polar lipids were separated in a Kinetex EVO C18 column 2.6 µm, 2.1 mm x 100 mm (Phenomenex). The mobile phase consisted of A: water, B: methanol and C: 2-propanol containing 10 mM ammonium formate +0.1% formic acid, at a flow rate of 0.6 mL/min. The gradient used was as follows: 0 min, 10% B, 40% C; 0.5 min, 10% B, 50% C; 1.5 min, 9.5% B, 52.5% C; 1.6 min, 7.5% B, 63.5% C; 5 min, 7% B, 66.5% C; 5.1 min, 4% B, 82.5% C; 7.5 min, 3.5% B, 85% C; 9 min, 3.5% B, 85% C; 9.5 min, 0% B, 100% C; 11.5 min, 0% B, 100% C; 11.6 min, 10% B, 40% C. A post run of 2 min in initial conditions was used for column conditioning.

Metabolites were quantified using Mass Hunter Quantitative Analysis B.07.00 (Agilent Technologies). Lipid characterization was done by matching their accurate mass and isotopic distributions to the Metlin-PCDL database (Scripps Research

Institute, La Jolla, CA, USA) allowing a mass error of 10 ppm and a score higher than 80 for isotopic distribution.

2.3. Statistical analyses

Statistical assessments were performed with the R program (RStudio version 4.0.5). The MetaboAnalystR package was used to generate scores and loading plots and included False Discovery Rates (FDR), Volcano plots, Principal Component Analysis (PCA), Partial Least Square Discriminant Analysis (PLS-DA), and hierarchically clustered heatmaps [30]. To evaluate the diagnostic accuracy of different combinations of lipids, we constructed a Monte Carlo cross validation model that combined from 5 to 100 random variables, and subsequently calculated the area under the curve of the Receiver Operating Characteristics (ROC) curves, and confusion matrices [31]. The TableOne package was used to generate mean and standard deviation of all lipid concentrations [32]. The R-commands employed are shown as Supplementary Methods (Supplementary_Materials.docx file).

3. Results

3.1. Clinical characteristics of the studied groups

The clinical characteristics of all participants are shown in Table 1. COVID-19-negative patients were significantly older and consumed less alcohol than the control group. COVID-19-positive patients had a lower frequency of smoking habit, alcohol intake, type 2 diabetes mellitus, chronic kidney disease and cancer than COVID-19-negative patients. The McCabe score and the Charlson index indicated that COVID-19-positive patients were, in general, less severe than COVID-19-negative patients.

3.2. Acylcarnitines, arachidonic acid and oxylipins: The common lipid signature of COVID-19-positive and COVID-19-negative patients

Numerical results are shown in Supplementary Tables (Supplementary_Tables.xls file). Volcano plots identified changes in the concentrations of 107 species comparing the COVID-19-positive patients vs. the healthy volunteers and 108 species comparing the COVID-19-negative patients vs. the healthy volunteers. The species with the greatest changes were O-octanoyl-R-carnitine (CAR 8:0) and LPE,

which were increased, and the oxylipins 9/13-hydroxyoctadecadienoic acid (9-HODE/13-HODE) and 15-HETE which were decreased (Fig. 1A). The heatmap clustering algorithm grouped the lipids into four blocks: The first three blocks were constituted mainly by oxylipins and the fourth by bile acids (Fig. 1B). PCA and PLS-DA completely segregated the populations of healthy volunteers from COVID-19 patients (either positive or negative), and the Variable Importance in Projection (VIP) score identified 9-HODE/13-HODE and 15-HETE as the most effective lipids in distinguishing the groups of patients from the healthy volunteers (Fig. 1C and D). We did not observe any significant differences between the position of the fatty acid chain of the lysophospholipids (LPC and LPE) in the different study groups (Supplementary Fig. 1).

The enrichment analysis showed an alteration of the pathways of fatty acid synthesis, the metabolism of arachidonic, linoleic and linolenic acids (precursors of oxylipins), and the □-oxidation of fatty acids in COVID-19-positive or COVID-19-negative patients compared to control subjects (Fig. 2A and B).

Monte Carlo models were generated to help identify those species that could be useful as biomarkers of infectious/inflammatory processes (whether COVID-19-positive or not). The models initially combined five randomly chosen lipid species and determined the area under the curve (AUC) for each from the combined ROC curve. The numbers of variables were progressively increased to 100 in 6 different models. In all instances, the analyses of the AUC-ROC curves were >0.98 (Fig. 3A). The 100-variable model was chosen to construct a confusion matrix, which correctly classified all but 1 of the patients (Fig. 3B). The algorithm identified oxylipins as the most relevant variables in the construction of the model. Other species identified were carnitines and lysophospholipids (Fig. 3C). From among these species, we chose arachidonic acid for further analysis because: its physiological and pathological importance is high; it is one of the main precursors of oxylipin synthesis; its internal standard is commercially available so its quantification is facilitated. Figure 3D shows serum concentrations of arachidonic acid being significantly decreased in COVID-19-positive as well as COVID-19-negative patients. Moreover, the AUCs of the ROC curves for arachidonic acid were >0.97 in the discrimination of both patient groups from the control group (Fig. 3E).

3.3. Phosphatidylcholines and secondary bile acids are specifically altered in COVID-19 positive patients

Volcano plots identified changes in the concentrations of 86 species comparing the COVID-19-positive *vs.* COVID-19-negative patients (78 increased and 8 decreased in COVID-19-positive patients). The species that presented greatest changes were phosphatidylcholine 36:5 (PC 36:5), long-chain triglycerides (TG) 54:2 and 54:7 which were increased, and carnitine (CAR) 18:2, epoxystearic acid, and glycodeoxycholic acid, that were decreased in COVID-19-positive patients (Fig. 4A). PCA and PLS-DA showed separation but with a certain degree of overlap (Fig. 4B). The most relevant parameters in the discrimination between both groups of patients were the secondary bile acids deoxycholic acid and ursodeoxycholic/hyodeoxycholic acid (Fig. 4C). The heatmap clustered TG and PC values into two different groups, although with very similar behavior: they tended to be relatively more concentrated in COVID-19-positive patients than in the COVID-19-negative patients (Fig. 4D).

As in the previous section (described above), we generated Monte Carlo models to ascertain whether there was a biological marker that effectively discriminated between COVID-19-positive and COVID-19-negative patients (Supplementary Fig. 2A and B). The approach identified a variety of compounds, the concentrations of which differed in positive and negative patients (Supplementary Fig. 2C), but the AUC of even the best ROC curve did not exceed 0.8 (Supplementary Fig. 3D and 3E). Because the discriminatory ability of the Monte Carlo approach was modest, we manually tested the individual discriminatory ability of each of the variables; an AUC of 0.95 was obtained with the combination of LPC22:6-sn2 and PC36:1 (Fig. 4E).

3.4. Lipid profile in COVID-19-positive patients was related to specific comorbidities but not to clinical prognosis or survival

When we analyzed the lipid profile in relation to individual comorbidities, we observed several important differences. For example, patients with cancer had significantly higher levels of most lipid series than those patients without cancer, while patients with chronic lung disease had, in general, lower lipid levels (Fig. 5A). However, this analysis should be viewed with caution since most of the patients had more than

one comorbidity and, as such, we prefer not to speculate on the influence of their interactions. To evaluate whether alterations in the lipid profile could be used to predict disease severity or mortality we applied K-means clustering in order to group patients according to their similarities within the circulating lipidome (Fig. 5B). All the distributions were dispersed and overlapped to a considerable extent, indicating that there was no significant relationship between lipid profile and survival, admission to the ICU, or the Charlson and McCabe indices.

We did not find any significant influence of sex differences or potentially inflammatory cardiometabolic comorbidities (cardiovascular disease or type 2 diabetes mellitus) on the lipidomic signature neither in COVID-19-positive nor in COVID-19-negative patients. Both PCA and heatmap clustering showed a considerable overlap in groups (Supplementary Figures 3 and 4).

4. Discussion

When we compared the results of the COVID-19-positive patients with the healthy volunteers, the most relevant findings were the increases in the concentrations of CAR 8:0 and LPE, and the decrease in the concentrations of 9/13-HODE and 15-HETE. The enrichment analysis identified alterations in the synthesis pathway of arachidonic acid from fatty acids. The measurement of the serum levels of arachidonic acid showed a high level of discrimination between patients and control subjects. Increased serum CAR 8:0 concentrations in COVID-19-positive patients may be a reflection of mitochondrial dysfunction. Acylcarnitines are markers of mitochondrial function, specifically for β-oxidation of fatty acids. They are synthesized via carnitine palmitoyltransferase 1 that ferries fatty acids into the mitochondrial matrix. Incomplete fatty acid oxidation results in elevated acylcarnitine concentrations [33]. Indeed, our enrichment analysis suggested alterations in the pathways of mitochondrial β-oxidation of very-long-chain and medium-chain fatty acids. The mitochondrial long-chain fatty acids β-oxidation is impaired in several viral infections, including COVID-19 [34], while β-oxidation defects are mirrored by changes in the concentration of long-chain acylcarnitines. The accumulation of acylcarnitines within the lung has been reported to be a risk factor for acute lung injury due to their inhibition of pulmonary surfactants [35].

Fatty acids play essential roles in viral infection because they provide building blocks for membrane synthesis during virus proliferation, and also because fatty acids can be converted to many lipid mediators such as the eicosanoids, which play significant roles in immune and inflammatory responses [36]. We observed decreased serum concentrations of several fatty acids including arachidonic, stearic, lauric, and palmitic acid in COVID-19-positive patients compared with healthy individuals. This decrease may be related to enhanced synthesis pathways of viral membrane phospholipids. Among the fatty acids, the most marked alteration that we observed was a highly significant decrease in serum arachidonic acid concentration. This finding confirms an earlier study [37]. This may be relevant from a pathophysiological point of view in that arachidonic acid is a potent antiviral agent participating in the inactivation of enveloped viruses, including SARS-CoV-2 [10]. A decrease in the concentrations of this lipid would be detrimental to the host, and would encourage the survival of the invading virus. A further study reported that exogenous supplementation with arachidonic acid inhibited HcoV-229E virus replication in cultured cells [38]. The decrease in circulating levels of fatty acids was associated with a decrease in the concentrations of 9/13-HODE and 15-HETE; oxylipin products of oxidation of linoleic acid and arachidonic acid, respectively. We would have expected to find increased serum oxylipin levels because their concentrations tend to increase with oxidative stress and because they are mediators of the inflammatory response [39]. However, an early study showed that high levels of oxylipins in lung cells infected by COVID-19 do not correspond to any concomitant increases in their concentrations in the circulation [40]. Indeed, these lipids are transported in plasma associated, mainly, with high-density lipoproteins from which they can be degraded by the antioxidant enzyme paraoxonase-1 [24,41].

Although the alterations in the lipid signature of COVID-19-positive patients are fairly unambiguous when compared to healthy subjects, COVID-19-negative patients presented similar alterations, as well. This finding suggests that these alterations were not specific to SARS-CoV-2 infection but, rather, are common to a multitude of infectious/inflammatory processes. For this reason, we compared the lipidomic signature of the COVID-19-positive patients with that of the COVID-19-negative patients. One alteration in particular was the significant difference in the circulating

levels of PC and LPC. Several studies have proposed a role of these molecules in COVID-19 infection, but the results published are far from consistent. Three studies had showed a decrease in plasma PC and an increase in LPC levels in COVID-19-positive patients compared to healthy subjects [42-44] while others showed that both phospholipids decreased [45,46], or even that the concentrations of PC increased [14] and those of LPC decreased [47]. We found a decrease in the serum concentration of LPC 22:6 and an increase in that of PC 36:1 and, hence, the ratio between the two phospholipids discriminated fairly well between positive and negative patients, and with excellent diagnostic accuracy. In addition, Volcano plots identified PC 36:5 as one of the lipid species that was most strongly increased when comparing positive *vs.* negative patients. These results agree with those reported in Calu-3 cells, where an increase in PC synthesis was observed when the cells were infected with SARS-CoV-2 [48]. Differences between the characteristics of the patient groups studied can probably explain this discrepancy between different authors' findings. Thus, some studies have been performed in severely affected patients with pneumonia [44] or critically ill [45], others in asymptomatic patients [47], and others in patients with various levels of severity [42-44]. Moreover, in all of them the lipidomic signatures had been compared with those of healthy volunteers. Our approach is unique in that we compared COVID-19 patients with patients with infectious/inflammatory diseases of origins other than COVID-19 infection.

Several factors could influence plasma PC and LPC concentrations. For example, both are key components of cell membranes and lipoproteins. Low plasma levels of these compounds may be explained as resulting from liver impairment in patients with severe COVID-19, while their increase would suggest increased activity of phospholipase A_2 [48]. Alterations in PC and LPC levels have been related to disease severity because of the roles that these lipids play in the inflammatory response [49].

Another alteration we observed in the COVID-19-positive patients when compared with the COVID-19-negative patients was a decrease in the concentrations of secondary bile acids, mainly deoxycholic acid and ursodeoxycholic/hyodeoxycholic acid; products of metabolism in the human gut microbiome. Our results are in accordance with those reporting that the fecal microbiome diversity is decreased in COVID-19 patients [50] and SARS-CoV-2-infected primates [17]. Moreover, decreased

plasma deoxycholic concentrations have been reported in severe COVID-19 patients compared to those with milder forms of the disease [51]. Inflammation caused by lung infection can disrupt the gut barrier integrity and increase the permeability to gut microbes and microbial products. This microbial translocation can exacerbate inflammation resulting from positive feedback. Further, microbial translocation may also modulate the circulating levels of gut microbiota-associated products such as secondary bile acids. As such, the circulating levels of these compounds would reflect the functional status of the gut and the metabolic activity of its microbiota [52]. Also, they are biologically active molecules that regulate several immunological functions, including inflammatory responses. Indeed, ursodeoxycholic acid has antioxidant, anti-inflammatory, anti-apoptotic, and immunomodulatory properties [16]. However, a disruption in the interaction between the gut and the lung has been related to respiratory tract diseases with causes other than COVID-19 [53], which suggests that secondary bile acid measurements are only useful when comparing COVID-19 infected patients and patients with non-respiratory inflammatory/infectious diseases.

We did not find any significant difference in the lipidomic signature of patients who survived and those who did not, nor with admission to the ICU, nor in the clinical prognosis. In this sense we differ from earlier studies, albeit the published information is scarce. For example, Siendones et al. [49] found that a panel of 22 metabolites (including PC and LPC), predicted disease severity (as measured as a need for ICU admission). Giron et al. [51] reported that alterations in secondary bile acid levels, resulting from disrupted crosstalk between gut and lung, are associated with ICU admission. The reasons for these discrepancies are purely speculative. Plausible explanations could be the heterogeneity of the disease itself, the different levels of severity and, as well, the associated comorbidities in the groups of patients studied by the different authors.

We are unable to provide realistic explanations regarding the extent to which variations in the serum lipidome reflect alterations in the affected tissues. Lipid metabolism is complex and can be affected by multiple factors. In particular, it is difficult to discern from measurements made in single plasma samples which tissue is affected in specific disease and what is the mechanism underlying the alteration [54]. However, some interesting hypotheses can be formulated. For example, the lipidome

of the different types of lung cells in humans has been characterized [55], and significant variations have been found in different lipid subclasses and, in particular, in the length of the fatty acid chains. Thus, lung immune cells are relatively richer in long-chain TG that are supposed to have a regulatory role in the immune response, as signal molecules. Indeed, long-chain TG are a source of polyunsaturated fatty acids that, due to the action of oxidative stress, can give rise to bioactive lipid mediators that regulate inflammation and the immune response [56,57]. Our study found a significant, and very relevant, increase in serum long-chain TG concentrations in COVID-19-positive compared with COVID-19-negative patients. TG are carried in the circulation packed in the very-low density lipoproteins (VLDL), and studies agree in that the levels of triglycerides, VLDL, and polyunsaturated fatty acids are increased in COVID-19 and Ebola virus disease [23,58-60]. Therefore, this elevation in long-chain TG concentrations could be related to the immune response, although the mechanisms behind its deregulation are not well elucidated.

In summary, lipidomics and machine learning provide cost- and time-effective biomarker detection for COVID-19 infection. They define altered biochemical pathways and possible therapeutic targets. We identified CAR, LPE, arachidonic acid and oxylipins as the most altered parameters in COVID-19 patients compared to healthy volunteers. However, our study is also a cautionary note in that it shows these alterations to be not confined to COVID-19, and appear to occur in other diseases with an infectious/inflammatory component. We also identified long-chain TG, PC36:5, LPC22:6-sn2, PC36:1 and secondary bile acids as the most altered parameters when comparing COVID-19-positive versus COVID-19-negative patients. These lipid alterations highlight the options of continuing to treat these patients post-discharge from hospital. Given the pro-atherogenic role of some of these lipid species, follow-up treatment could include lifestyle modifications and lipid-lowering drugs. Moreover, we found that arachidonic acid and the ratio between LPC22:6-sn2 and PC36:1 show an excellent diagnostic accuracy (AUC from the ROC curves >0.95) in discriminating COVID-19-positive from healthy subjects and COVID-19-negative patients, respectively.

Our study has several limitations: Firstly, the number of cases studied is small, especially in the groups of healthy volunteers and COVID-19-negative patients. All of our patients were hospitalized and, therefore, we do not know the degree of alteration

of the lipid signature in COVID-19-positive patients who are asymptomatic or have mild symptoms. The COVID-19-negative patients were a heterogeneous group, with different types of underlying diseases, albeit they enabled us to identify specific alterations of COVID-19 or, at least, of severe respiratory diseases. Finally, our semi-targeted approach allowed us to measure accurately those species of analytes for which we had standards. However, the accuracy of measurements of the rest of the species are, inevitably, somewhat lower. Nevertheless, our systematic investigation showed that the integration of lipidomics with machine learning algorithms can increase the understanding of COVID-19 pathophysiology and, as such, facilitate more effective clinical decision making.

CRediT authorship contribution statement

Helena Castañé: Conceptualization, Methodology, Software, Formal analysis, Investigation, Data curation, Writing-Original draft preparation. **Simona Iftimie:** Conceptualization, Methodology, Formal analysis, Investigation, Data curation, Writing-Original draft preparation. **Gerard Baiges-Gaya:** Methodology, Investigation. **Elisabet Rodríguez-Tomàs:** Methodology, Investigation. **Andrea Jiménez-Franco:** Methodology, Investigation. **Ana Belisa López-Azcona:** Formal analysis, Investigation, Data curation. **Pedro Garrido:** Formal analysis, Investigation, Data curation. **Antoni Castro:** Data curation, Funding acquisition. **Jordi Camps:** Conceptualization, Formal analysis, Supervision, Project administration, Writing-Review & Editing. **Jorge Joven:** Data curation, Funding acquisition.

Declaration of competing interest

The authors report no potential conflicts of interest relevant to this article.

Acknowledgments

The authors thank Dr. Peter R. Turner for critical review and language editing of the manuscript. The EURECAT-Technology Centre of Catalonia (Reus, Spain) contributed its expertise and advice in lipidomics measurements.

Funding

This work was supported by the *Fundació La Marató de TV3,* Barcelona, Spain [201807-10], the *Generalitat de Catalunya*, Barcelona, Spain [PERIS-SLT017/3501/2020 to H.C. and AGAUR 2020FI_d1 00215 to E.R.T.], and the *Instituto de Salud Carlos III*, Madrid, Spain [FI19/00097 to G.B.G.]. Funders had no role in the study design, data collection, data analysis, data interpretation, and writing the manuscript.

References

1. World Health Organization. Coronavirus disease (COVID-19) weekly epidemiological update and weekly operational update. Available at: . Accessed 25 January 2022.
2. Iftimie S, López-Azcona AF, Vicente-Miralles M, Descarrega-Reina R, Hernández-Aguilera A, Riu F, et al. Risk factors associated with mortality in hospitalized patients with SARS-CoV-2 infection. A prospective, longitudinal, unicenter study in Reus, Spain. PloS One. 2020;15:e0234452. doi: 10.1371/journal.pone.0234452. PMID: 32881860; PMCID: PMC7470256.
3. Iftimie S, López-Azcona AF, Vallverdú I, Hernández-Flix S, de Febrer G, Parra S, et al. First and second waves of coronavirus disease-19: A comparative study in hospitalized patients in Reus, Spain. PLoS One. 2021;16:e0248029. doi: 10.1371/journal.pone.0248029. PMID: 33788866; PMCID: PMC8011765.
4. Itelman E, Wasserstrum Y, Segev A, Avaky C, Negru L, Cohen D, et al. Clinical Characterization of 162 COVID-19 patients in Israel: Preliminary report from a large tertiary center. Isr Med Assoc J. 2020;22: 271-. PMID: 32378815.
5. Penlioglou T, Papachristou S, Papanas N. COVID-19 and diabetes mellitus: May old anti-diabetic agents become the new philosopher's stone? Diabetes Ther. 2020;11:1-3. doi: 10.1007/s13300-020-00830-0. PMID: 32382358; PMCID: PMC7204191.
6. Huang R, Zhu L, Xue L, Liu L, Yan X, Wang J, et al. Clinical findings of patients with coronavirus disease 2019 in Jiangsu province, China: A retrospective, multi-

center study. PLoS Negl Trop Dis. 2020;14: e0008280. doi: 10.1371/journal.pntd.0008280. PMID: 32384078; PMCID: PMC7239492.

7. Silva-Lagos LA, Pillay J, van Meurs M, Smink A, van der Voort PHJ, de Vos P. DAMpening COVID-19 severity by attenuating danger signals. Front Immunol. 2021;12:720192. doi: 10.3389/fimmu.2021.720192. PMID: 34456928; PMCID: PMC8397524.
8. Srivastava SP, Srivastava R, Chand S, Goodwin JE. Coronavirus disease (COVID)-19 and diabetic kidney disease. Pharmaceuticals (Basel). 2021;14: 751. doi: 10.3390/ph14080751. PMID: 34451848; PMCID: PMC8398861.
9. Xiao N, Nie M, Pang H, Wang B, Hu J, Meng X, et al. Integrated cytokine and metabolite analysis reveals immunometabolic reprogramming in COVID-19 patients with therapeutic implications. Nat Commun. 2021;12:1618. doi: 10.1038/s41467-021-21907-9 PMCID: PMC7955129.
10. Casari I, Manfredi M, Metharom P, Falasca M. Dissecting lipid metabolism alterations in SARS-CoV-2. Prog Lipid Res. 2021;82:101092. doi:10.1016/j.plipres.2021.101092 PMCID: PMC7869689
11. Theken KN, FitzGerald GA. Bioactive lipids in antiviral immunity. Science. 2021;371:237-8. doi: 10.1126/science.abf3192. PMID: 33446545.
12. Weigele BA, Orchard RC, Jimenez A, Cox GW, Alto NM. A systematic exploration of the interactions between bacterial effector proteins and host cell membranes. Nat Commun. 2017;8:532. doi: 10.1038/s41467-017-00700-7. PMID: 28912547; PMCID: PMC5599653.
13. Zhang Q, Xiang R, Huo S, Zhou Y, Jiang S, Wang Q, et al. Molecular mechanism of interaction between SARS-CoV-2 and host cells and interventional therapy. Signal Transduct Target Ther. 2021;6:233. doi: 10.1038/s41392-021-00653-w. PMID: 34117216; PMCID: PMC8193598.
14. Lam SM, Zhang C, Wang Z, Ni Z, Zhang S, Yang S, et al. A multi-omics investigation of the composition and function of extracellular vesicles along the temporal trajectory of COVID-19. Nat Metab. 2021;3:909-22. doi: 10.1038/s42255-021-00425-4. Epub 2021 Jun 22. PMID: 34158670.

15. Camps J, Castañé H, Rodríguez-Tomàs E, Baiges-Gaya G, Hernández-Aguilera A, Arenas M, et al. On the role of paraoxonase-1 and chemokine ligand 2 (C-C motif) in metabolic alterations linked to inflammation and disease. A 2021 update. Biomolecules. 2021;11:971. doi: 10.3390/biom11070971. PMID: 34356595; PMCID: PMC8301931.

16. Abdulrab S, Al-Maweri S, Halboub E. Ursodeoxycholic acid as a candidate therapeutic to alleviate and/or prevent COVID-19-associated cytokine storm. Med Hypotheses. 2020;143:109897. doi: 10.1016/j.mehy.2020.109897. PMID: 32505909; PMCID: PMC7261102.

17. Sokol H, Contreras V, Maisonnasse P, Desmons A, Delache B, Sencio V, et al. SARS- CoV-2 infection in nonhuman primates alters the composition and functional activity of the gut microbiota. Gut Microbes. 2021;13:1-19. doi: 10.1080/19490976.2021.1893113. PMID: 33685349; PMCID: PMC7951961.

18. Morita M, Kuba K, Ichikawa A, Nakayama M, Katahira J, Iwamoto R, et al. The lipid mediator protectin D1 inhibits influenza virus replication and improves severe influenza. Cell. 2013;153:112–25. doi: 10.1016/j.cell.2013.02.027. PMID: 23477864.

19. Lydic TA, Goo YH. Lipidomics unveils the complexity of the lipidome in metabolic diseases. Clin Transl Med. 2018;7:4. doi: 10.1186/s40169-018-0182-9. PMID: 29374337; PMCID: PMC5786598.

20. Kyle JE. How lipidomics can transform our understanding of virus infections. Expert Rev Proteomics. 2021;18:329-32. doi: 10.1080/14789450.2021.1929177. PMID: 34030561.

21. Mussap M, Fanos V. Could metabolomics drive the fate of COVID-19 pandemic? A narrative review on lights and shadows. Clin Chem Lab Med. 2021;Epub ahead of print. doi: 10.1515/cclm-2021-0414. PMID: 34332518.

22. Leier HC, Weinstein JB, Kyle JE, Lee JY, Bramer LM, Stratton KG, et al. A global lipid map defines a network essential for Zika virus replication. Nat Commun. 2020;11:3652. doi: 10.1038/s41467-020-17433-9. PMID: 32694525; PMCID: PMC7374707.

23. Kyle JE, Burnum-Johnson KE, Wendler JP, Eisfeld AJ, Halfmann PJ, Watanabe T, et al. Plasma lipidome reveals critical illness and recovery from human Ebola virus disease. Proc Natl Acad Sci USA. 2019;116:3919-28. doi: 10.1073/pnas.1815356116. Epub 2019 Feb 11. PMID: 30808769; PMCID: PMC6397561.

24. Iftimie S, García-Heredia A, Pujol I, Ballester F, Fort-Gallifa I, Simó JM, et al. Preliminary study on serum paraoxonase-1 status and chemokine (C-C motif) ligand 2 in hospitalized elderly patients with catheter-associated asymptomatic bacteriuria. Eur J Clin Microbiol Infect Dis. 2016;35:1417-24. doi: 10.1007/s10096-016-2679-8.

25. Fort-Gallifa I, García-Heredia A, Hernández-Aguilera A, Simó JM, Sepúlveda J, Martín-Paredero V, et al. Biochemical indices of oxidative stress and inflammation in the evaluation of peripheral artery disease. Free Radic Biol Med. 2016;97:568-76. doi: 10.1016/j.freeradbiomed.2016.07.011. PMID: 27449545.

26. McCabe WR, Jackson GG. Gram-negative bacteremia. I. Etiology and ecology. Arch Intern Med 1962;110:847-64.

27. Berkman LF, Leo-Summers L, Horwitz RI. Emotional support and survival after myocardial infarction. A prospective, population-based study of the elderly. Ann Intern Med. 1992;117:1003-9. doi: 10.7326/0003-4819-117-12-1003. PMID: 1443968.

28. Fernández-Arroyo S, Hernández-Aguilera A, de Vries MA, Burggraaf B, van der Zwan E, Pouw N, et al. Effect of Vitamin D3 on the postprandial lipid profile in obese patients: A non-targeted lipidomics study. Nutrients 2019;11:1194. doi: 10.3390/nu11051194 PMCID: PMC6567161.

29. Baiges-Gaya G, Fernández-Arroyo S, Luciano-Mateo F, Cabré N, Rodríguez-Tomàs E, Hernández-Aguilera A, et al. Hepatic metabolic adaptation and adipose tissue expansion are altered in mice with steatohepatitis induced by high-fat high-sucrose diet. J Nutr Biochem. 2021;89:108559. doi: 10.1016/j.jnutbio.2020.108559. PMID: 33264665.

30. Pang Z, Chong J, Li S, Xia J. MetaboAnalystR 3.0: Toward an optimized workflow for global metabolomics. Metabolites. 2020;10:186. doi: 10.3390/metabo10050186. PMID: 32392884; PMCID: PMC7281575.

31. Zweig MH, Campbell G. Receiver-operating characteristic (ROC) plots: a fundamental evaluation tool in clinical medicine. Clin Chem. 1993;39:561-77.

32. Panos A, Mavridis D. TableOne: an online web application and R package for summarising and visualising data. Evid Based Ment Health. 2020;23:127-30. doi: 10.1136/ebmental-2020-300162.

33. Mai M, Tönjes A, Kovacs P, Stumvoll M, Fiedler GM, Leichtle AB. Serum levels of acylcarnitines are altered in prediabetic conditions. PLoS One. 2013;8:e82459. doi: 10.1371/journal.pone.0082459 PMCID: PMC3863089.

34. Ayres JS. A metabolic handbook for the COVID-19 pandemic. Nat Metab. 2020;1-14. doi: 10.1038/s42255-020-0237-2. PMCID: PMC7325641.

35. Otsubo C, Bharathi S, Uppala R, Ilkayeva OR, Wang D, McHugh K, et al. Long-chain acylcarnitines reduce lung function by inhibiting pulmonary surfactant. J Biol Chem. 2015;290:23897-904. doi: 10.1074/jbc.M115.655837 PMCID: PMC4583047.

36. Bennett M, Gilroy DW. Lipid mediators in inflammation. In: Gordon S. Myeloid Cells in Health and Disease. Hoboken, USA: ASM Press; 2016:343-366.

37. Shen B, Yi X, Sun Y, Bi X, Du J, Zhang C, et al. Proteomic and metabolomic characterization of COVID-19 patient sera. Cell. 2020; 182:59-72.e15. doi: 10.1016/j.cell.2020.05.032. PMID: 32492406; PMCID: PMC7254001.

38. Yan B, Chu H, Yang D, Sze KH, Lai PM, Yuan S, et al. Characterization of the lipidomic profile of human coronavirus-infected cells: Implications for lipid metabolism remodeling upon coronavirus replication. Viruses. 2019;11:73. doi: 10.3390/v11010073. PMID: 30654597; PMCID: PMC6357182.

39. Leghmar K, Cenac N, Rolland M, Martin H, Rauwel B, Bertrand-Michel J, et al. Cytomegalovirus infection triggers the secretion of the PPARγ agonists 15-hydroxyeicosatetraenoic acid (15-HETE) and 13-hydroxyoctadecadienoic acid (13-HODE) in human cytotrophoblasts and placental cultures. PLoS One. 2015;10: e0132627. doi: 10.1371/journal.pone.0132627 PMCID: PMC4501751.

40. Archambault AS, Zaid Y, Rakotoarivelo V, Turcotte C, Doré E, Dubuc I, et al. High levels of eicosanoids and docosanoids in the lungs of intubated COVID-19 patients FASEB J. 2021;35:e21666. doi: 10.1096/fj.202100540R PMCID: PMC8206770

41. Rodríguez-Tomàs E, Iftimie S, Castañé H, Baiges-Gaya G, Hernández-Aguilera A, González-Viñas M, et al. Clinical performance of paraoxonase-1-related variables and novel markers of inflammation in coronavirus disease-19. A machine learning approach. Antioxidants (Basel). 2021;10: 991. doi: 10.3390/antiox10060991 PMCID: PMC8234277

42. Wu D, Shu T, Yang X, Song JX, Zhang M, Yao C, et al. Plasma metabolomic and lipidomic alterations associated with COVID-19. Natl Sci Rev. 2020;7:1157-68. doi: 10.1093/nsr/nwaa086. PMID: 34676128; PMCID: PMC7197563.

43. Song JW, Lam SM, Fan X, Cao WJ, Wang SY, Tian H, et al. Omics-driven systems interrogation of metabolic dysregulation in COVID-19 pathogenesis. Cell Metab. 2020;32:188-202.e5. doi: 10.1016/j.cmet.2020.06.016. PMID: 32610096; PMCID: PMC7311890.

44. Barberis E, Timo S, Amede E, Vanella VV, Puricelli C, Cappellano G, et al. Large-scale plasma analysis revealed new mechanisms and molecules associated with the host response to SARS-CoV-2. Int J Mol Sci. 2020;21:E8623. doi: 10.3390/ijms21228623. PMID: 33207699; PMCID: PMC7696386.

45. Fraser DD, Slessarev M, Martin CM, Daley M, Patel MA, Miller MR, et al. Metabolomics profiling of critically ill coronavirus disease 2019 patients: identification of diagnostic and prognostic biomarkers. Crit Care Explor. 2020;2: e0272. doi: 10.1097/CCE.0000000000000272. PMID: 33134953; PMCID: PMC7587450.

46. Delafiori J, Navarro LC, Siciliano RF, de Melo GC, Busanello ENB, Nicolau JC, et al. Covid-19 automated diagnosis and risk assessment through metabolomics and machine learning. Anal Chem. 2021;93:2471-9. doi: 10.1021/acs.analchem.0c04497. Epub 2021 Jan 20. PMID: 33471512; PMCID: PMC8023531.

47. Hao Y, Zhang Z, Feng G, Chen M, Wan Q, Lin J, et al. Distinct lipid metabolic dysregulation in asymptomatic COVID-19. iScience. 2021;24:102974. doi: 10.1016/j.isci.2021.102974. PMID:34396083; PMCID: PMC8356725.

48. Dissanayake TK, Yan B, Ng AC, Zhao H, Chan G, Yip CC, et al. Differential role of sphingomyelin in influenza virus, rhinovirus and SARS-CoV-2 infection of Calu-3 cells. J Gen Virol. 2021;102:001593. doi: 10.1099/jgv.0.001593. PMID: 33956593.

49. Sindelar M, Stancliffe E, Schwaiger-Haber M, Anbukumar DS, Adkins-Travis K, Goss CW, et al. Longitudinal metabolomics of human plasma reveals prognostic markers of COVID-19 disease severity Cell Rep Med. 2021;2:100369. doi: 10.1016/j.xcrm.2021.100369 PMCID: PMC8292035.

50. Ren Z, Wang H, Cui G, Lu H, Wang L, Luo H, et al. Alterations in the human oral and gut microbiomes and lipidomics in COVID-19. Gut. 2021; 70:1253-65. doi: 10.1136/gutjnl-2020-323826 PMCID: PMC8042598

51. Giron LB, Dweep H, Yin X, Wang H, Damra M, Goldman AR, et al. Plasma markers of disrupted gut permeability in severe COVID-19 patients. Front Immunol. 2021; 12:686240. doi: 10.3389/fimmu.2021.686240. Correction in: Front Immunol. 2021;12:779064. PMCID: PMC8219958.

52. Mayneris-Perxachs J, Fernandez-Real JM. Exploration of the microbiota and metabolites within body fluids could pinpoint novel disease mechanisms. FEBS J. 2020;287:856-65. doi: 10.1111/febs.15130. PMID: 31709683.

53. Dumas A, Bernard L, Poquet Y, Lugo-Villarino G, Neyrolles O. The role of the lung microbiota and the gut-lung axis in respiratory infectious diseases. Cell Microbiol. 2018;20:e12966. doi: 10.1111/cmi.12966. PMID: 30329198.

54. Jain M, Ngoy S, Sheth SA, Swanson RA, Phee EP, Liao R, et al. A systematic survey of lipids across mouse tissues. Am J Physiol Endocrinol Metab. 2014;306:E854-68. doi: 10.1152/ajpendo.00371.2013. PMID: 24518676. PMCID: PMC3989739.

55. Kyle JE, Clair G, Bandyopadhyay G, Misra RS, Zink EM, Bloodsworth KJ, et al. Cell type-resolved human lung lipidome reveals cellular cooperation in lung function. Sci Rep. 2018;8:13455. doi: 10.1038/s41598-018-31640-x. PMID: 30194354; PMCID: PMC6128932.

56. Dichlberger A, Kovanen PT, Schneider WJ. Mast cells: from lipid droplets to lipid mediators. Clin Sci (Lond). 2013;125:121-30. doi:10.1042/CS20120602. PMID: 23577635; PMCID: PMC3631086.

57. Dichlberger A, Schlager S, Maaninka K, Schneider WJ, Kovanen PT. Adipose triglyceride lipase regulates eicosanoid production in activated human mast cells. J Lipid Res. 2014;55:2471-8. doi: 10.1194/jlr.M048553. PMID: 25114172; PMCID: PMC4242440.

58. Nguyen M, Bourredjem A, Piroth L, Bouhemad B, Jalil A, Pallot G, et al. High plasma concentration of non-esterified polyunsaturated fatty acids is a specific feature of severe COVID-19 pneumonia. Sci Rep. 2021;11:10824. doi: 10.1038/s41598-021-90362-9. PMID: 34031519; PMCID: PMC8144366.

59. Bizkarguenaga M, Bruzzone C, Gil-Redondo R, Sanjuan I, Martin-Ruiz I, Barriales D, et al. Uneven metabolic and lipidomic profiles in recovered COVID-19 patients as investigated by plasma NMR metabolomics. NMR Biomed. 2022;35:e4637. doi: 10.1002/nbm.4637. Epub 2021 Oct 27. PMID: 34708437; PMCID: PMC8646702.

60. Bruzzone C, Bizkarguenaga M, Gil-Redondo R, Diercks T, Arana E, García de Vicuña A, et al. SARS-CoV-2 Infection dysregulates the metabolomic and lipidomic profiles of serum. iScience. 2020;23:101645. doi: 10.1016/j.isci.2020.101645. Epub 2020 Oct 5. PMID: 33043283; PMCID: PMC7534591.

Figure legends

Fig. 1. Lipid signatures differentiate COVID-19 positive and COVID-19-negative patients from healthy individuals. (A): Volcano plots representing the log fold-change of lipid species in COVID-19-positive (upper panel) and COVID-19-negative (lower panel) patients relative to the control group. (B): Heatmap showing the 15 most relevant lipid species in the control group (blue), COVID-19-negative (yellow) and COVID-19-positive (red) patients. (C): From left to right: Principal Component Analysis (PCA) clustering of the COVID-19-positive patients and the control group; Principal Least Square Discriminant Analysis (PLS-DA) clustering the COVID-19-positive patients and the control group; Variable Importance in Projection (VIP) score identifying 9/13-HODE and

15-HETE as the most relevant parameters discriminating between COVID-19-positive patients and the control group. (D): From left to right: PCA clustering the COVID-19-negative patients and the control group; PLS-DA clustering the COVID-19-negative patients and the control group; VIP score identifying 9/13-HODE and 15-HETE as the most relevant parameters discriminating between COVID-19-negative patients and the control group. In 3-dimensional plots of PCA and PLS-DA, each ball represents a patient, and positions depend on differences in lipid concentrations. Axes are formed by different combinations of variables, and the percentages represent the proportion of variance that can be explained. PCA is a non-supervised test and PLS-DA is a supervised analysis.

Acronyms: CAR: Acylcarnitine; DHEA: dehydroepiandrosterone; DHOME: dihydroxyoctadecenoic acid; HDHA: hydroxydocosahaxaenoic aid; HETE: hydroxyeicosatetraenoic acid; HODE: hydroxyoctadecadienoic acid; LPC: lysophosphatidylcholine; LPE: lysophosphatidylethanolamine; TG: triglyceride.

Fig. 2. Enrichment analysis showing the most severely affected biochemical pathways in COVID-19-positive patients (A) and COVID-19-negative patients (B) compared with the control group.

Fig. 3. Identification of biomarkers for infectious/inflammatory processes. (A): Receiver Operating Characteristics plot of Monte Carlo models corresponding to the combination of 5 to 100 variables. (B): Confusion matrix of the generated 100-variable model. (C): Relative importance of the different variables chosen by the model. (D) Serum arachidonic acid concentrations in the COVID-19-positive and COVID-19-negative patients and the control group. (D): Receiver Operating Characteristics plots of the measured arachidonic acid in discriminating between the selected groups.

Acronyms: AUC: Area under the curve; CAR: acylcarnitine; DHEA: dehydroepiandrosterone; HDHA: hydroxydocosahaxaenoic aid; HETE: hydroxyeicosatetraenoic acid; HODE: hydroxyoctadecadienoic acid; LPC: lysophosphatidylcholine; THOME: trihydroxyoctadecenoic acid.

Fig. 4. Lipid signatures differentiate between COVID-19-positive and COVID-19-negative patients. (A): Volcano plot representing the log fold-change of lipid species in COVID-19-positive with respect to COVID-19-negative patients. (B): Principal Component Analysis (PCA) clustering the COVID-19-positive and the COVID-19-negative patients. (C): Principal Least Square Discriminant Analysis (PLS-DA) clustering the COVID-19-positive and the COVID-19-negative patients. The Variable Importance in Projection (VIP) score identified deoxycholic and ursodeoxycholic/hyodeoxycholic acids as highly relevant parameters in the discrimination between both groups of patients. (D): Heatmap. (E): Serum concentrations of the selected lipid species in COVID-19-positive and COVID-19-negative patients, and Receiver Operating Characteristics plot of the ratio between them. In 3-dimensional plots of PCA and PLS-DA, each ball represents a patient, and position depends on differences in lipid concentrations. Axes are formed by different combination of variables, and percentages represent the proportion of variance that can be explained. PCA is a non-supervised test and PLS-DA is a supervised analysis.
Acronyms: AUC: Area under the curve; CAR: acylcarnitine; LPC: lysophosphatidylcholine; PC: phosphatidylcholine; TG: triglyceride.

Fig. 5. Relationships between the lipidomics signature and the clinical characteristics of COVID-19-positive patients. (A): Heatmap showing the variations in serum lipid concentrations in relation to comorbidities. (B): K-means clustering of patient group according to their similarities in the circulating lipidome. Each individual patient is represented by a point with a different color depending on whether or not they had the selected characteristic.
Acronyms: CAR: acylcarnitines; CE: cholesterol esters; DG: diglycerides; FA: fatty acids; LPC: lysophosphatidylcholines; LPE: lysophosphatidylethanolamines; PC: phosphatidylcholines; SM: sphingomyelins; TG: triglycerides.

Table 1. Demographic and clinical characteristics of the patients and the healthy subjects

		Healthy subjects n = 50	COVID-19 negative patients n = 45	COVID-19 positive patients n = 126	*P* value *	*P* value †
Demographic variables						
Age, years		75 (66- 84)	84 (75- 89)	71 (58-83)	< 0.001	< 0.001
Sex, male		38 (76.0)	30 (66.7)	68 (54.8)	0.218	0.112
Smoking, n (%)		19 (38.0)	16 (35.6)	6 (4.8)	0.834	0.076
Alcohol intake, n (%)		28 (56.0)	7 (15.5)	6 (4.8)	< 0.001	0.063
Comorbidities						
Cardiovascular Disease, n (%)		0	18 (40)	63 (54	NA	0.075
Type 2 Diabetes Mellitus, n (%)		0	22 (48.9)	30 (23.8)	NA	< 0.001
Chronic Neurological Disease n (%),		0	0	29 (23.0)	NA	NA
Chronic Kidney Disease, n (%)		0	19 (42.2)	22 (17.5)	NA	0.001
Chronic Lung Disease, n (%)		0	0	18 (14.3)	NA	NA
Cancer, n (%)		0	17 (37.8)	16 (12.7)	NA	< 0.001
Chronic Liver Disease, n (%)		0	0	1 (0.8)	NA	NA
McCabe index	RFD, n (%)	NA	10 (22.2)	7 (5.6)	NA	< 0.001
	UFD, n (%)		19 (42.2)	31 (24.6)		
	NFD, n (%)		16 (35.6)	88 (69.8)		
Charlson index	No comorbidity, n (%)	NA	10 (22.2)	83 (65.9)	NA	< 0.001
	Low comorbidity, n (%)		18 (40.0)	29 (23.0)		
	High comorbidity, n (%)		17 (37.8)	14 (11.1)		
Medications						
Oral antidiabetics, n (%)		NA	19 (42.2)	37 (29.4)	NA	0.083
Statins, n (%)		NA	16 (35.6)	44 (34.9)	NA	0.538
ACEIs, n (%)		NA	14 (31.1)	24 (27.0)	NA	0.364
ARAs, n (%)		NA	12 (26.7)	21 (16.7)	NA	0.109
Insulin, n (%)		NA	9 (20.0)	28 (22.2)	NA	0.468

* COVID-19 positive patients with respect to healthy subjects; † COVID-19 positive patients with respect to COVID-19 negative patients. Statistical analyses performed by the Student's *t* test (quantitative) or the χ-square test (qualitative). Results are given as medians and 95% CI or as numbers and percentages. ACEIs: Angiotensin converting enzyme inhibitors; ARAs, Angiotensin II receptor antagonists; NFD: Non-fatal disease; RFD: Rapidly fatal disease. UFD: Ultimately fatal disease

Highlights

- COVID-19 alters lipid metabolism of the infected host
- We evaluated serum lipidome in controls and patients with or without COVID-19
- A lipidomic signature differentiated patients from controls
- A lipidomic signature differentiated COVID-19 positive from negative patients

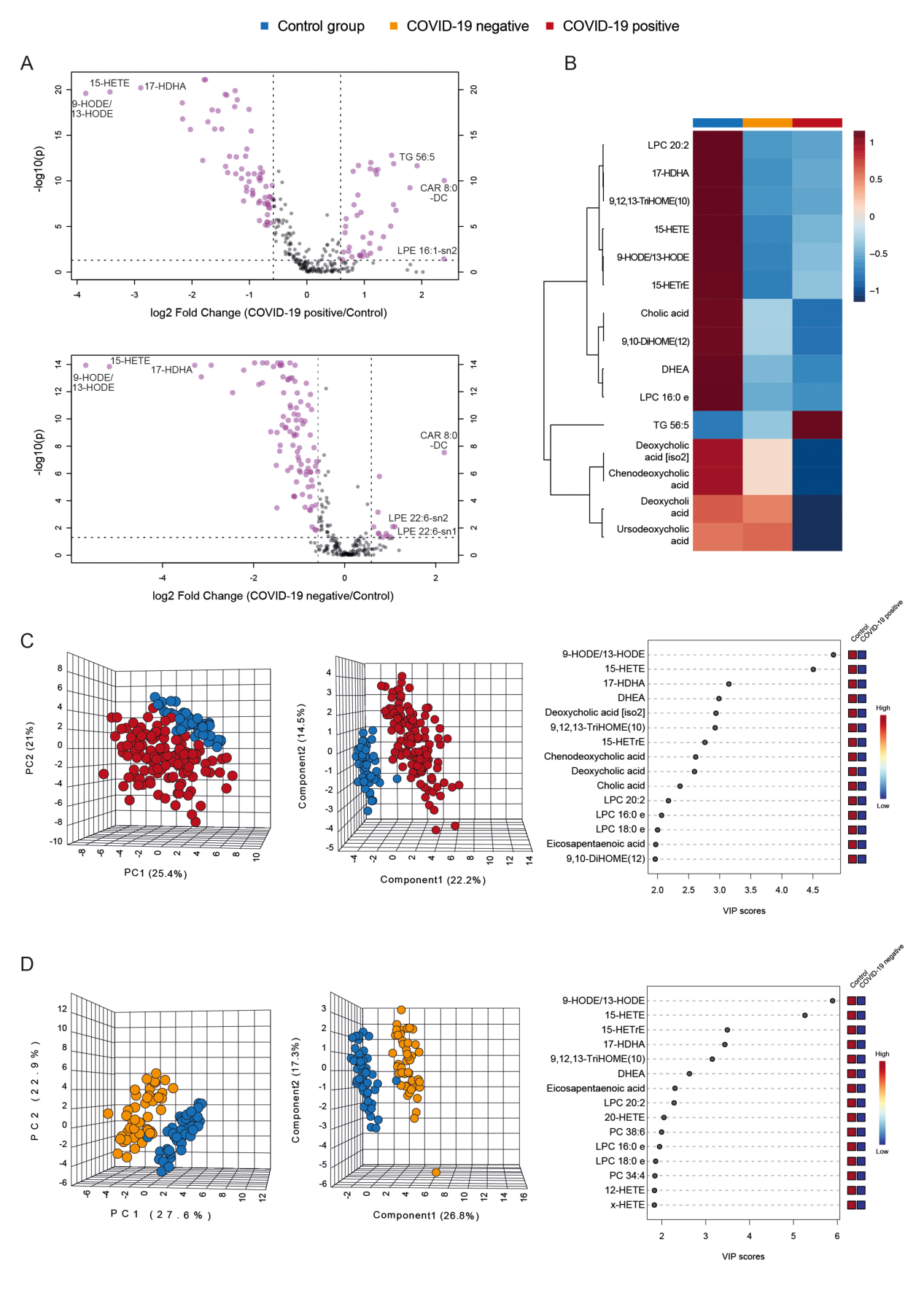
Control group
COVID-19 negative
COVID-19 positive
A
15-HETE
17-HDHA
9-HODE/
13-HODE
TG 56:5
CAR 8:0
-DC
LPE 16:1-sn2
-log10(p)
log2 Fold Change (COVID-19 positive/Control)
LPE 22:6-sn2
LPE 22:6-sn1
log2 Fold Change (COVID-19 negative/Control)
B
LPC 20:2
17-HDHA
9,12,13-TriHOME(10)
15-HETE
9-HODE/13-HODE
15-HETrE
Cholic acid
9,10-DiHOME(12)
DHEA
LPC 16:0 e
TG 56:5
Deoxycholic acid [iso2]
Chenodeoxycholic acid
Deoxycholi acid
Ursodeoxycholic acid
C
PC2 (21%)
PC1 (25.4%)
Component2 (14.5%)
Component1 (22.2%)
Control
COVID-19 positive
9-HODE/13-HODE
15-HETE
17-HDHA
DHEA
Deoxycholic acid [iso2]
9,12,13-TriHOME(10)
15-HETrE
Chenodeoxycholic acid
Deoxycholic acid
Cholic acid
LPC 20:2
LPC 16:0 e
LPC 18:0 e
Eicosapentaenoic acid
9,10-DiHOME(12)
High
Low
VIP scores
D
PC2 (22.9%)
PC1 (27.6%)
Component2 (17.3%)
Component1 (26.8%)
Control
COVID-19 negative
9-HODE/13-HODE
15-HETE
15-HETrE
17-HDHA
9,12,13-TriHOME(10)
DHEA
Eicosapentaenoic acid
LPC 20:2
20-HETE
PC 38:6
LPC 16:0 e
LPC 18:0 e
PC 34:4
12-HETE
x-HETE
High
Low
VIP scores

Figure 1

A

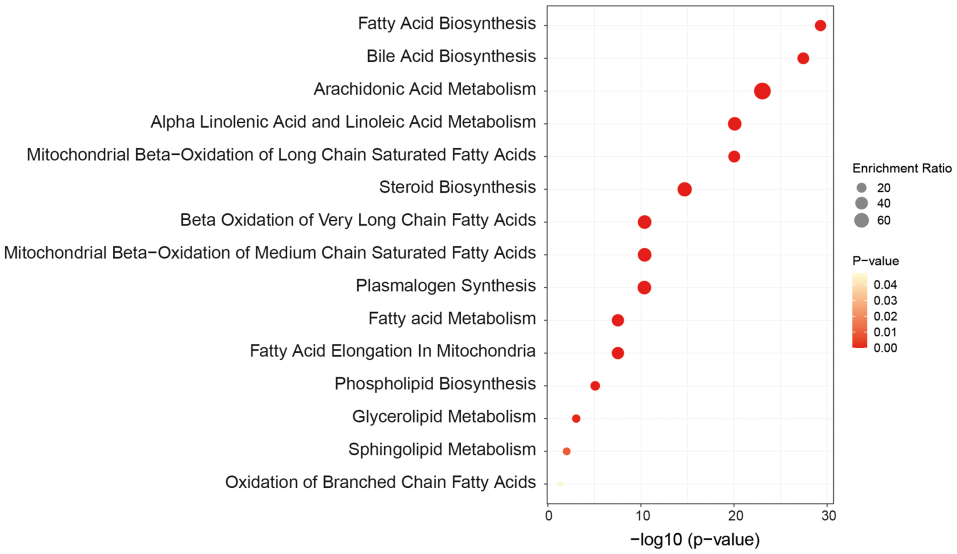
Fatty Acid Biosynthesis
Bile Acid Biosynthesis
Arachidonic Acid Metabolism
Alpha Linolenic Acid and Linoleic Acid Metabolism
Mitochondrial Beta−Oxidation of Long Chain Saturated Fatty Acids
Steroid Biosynthesis
Beta Oxidation of Very Long Chain Fatty Acids
Mitochondrial Beta−Oxidation of Medium Chain Saturated Fatty Acids
Plasmalogen Synthesis
Fatty acid Metabolism
Fatty Acid Elongation In Mitochondria
Phospholipid Biosynthesis
Glycerolipid Metabolism
Sphingolipid Metabolism
Oxidation of Branched Chain Fatty Acids
0
10
20
30
−log10 (p−value)
Enrichment Ratio
20
40
60
P−value
0.04
0.03
0.02
0.01
0.00

B

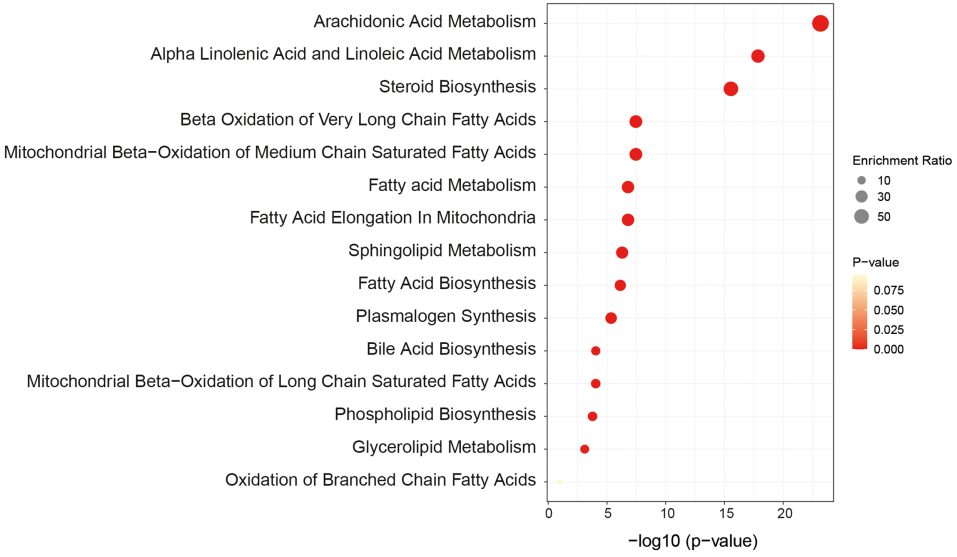
Arachidonic Acid Metabolism
Alpha Linolenic Acid and Linoleic Acid Metabolism
Steroid Biosynthesis
Beta Oxidation of Very Long Chain Fatty Acids
Mitochondrial Beta−Oxidation of Medium Chain Saturated Fatty Acids
Fatty acid Metabolism
Fatty Acid Elongation In Mitochondria
Sphingolipid Metabolism
Fatty Acid Biosynthesis
Plasmalogen Synthesis
Bile Acid Biosynthesis
Mitochondrial Beta−Oxidation of Long Chain Saturated Fatty Acids
Phospholipid Biosynthesis
Glycerolipid Metabolism
Oxidation of Branched Chain Fatty Acids
0
5
10
15
20
−log10 (p−value)
Enrichment Ratio
10
30
50
P−value
0.075
0.050
0.025
0.000

Figure 2

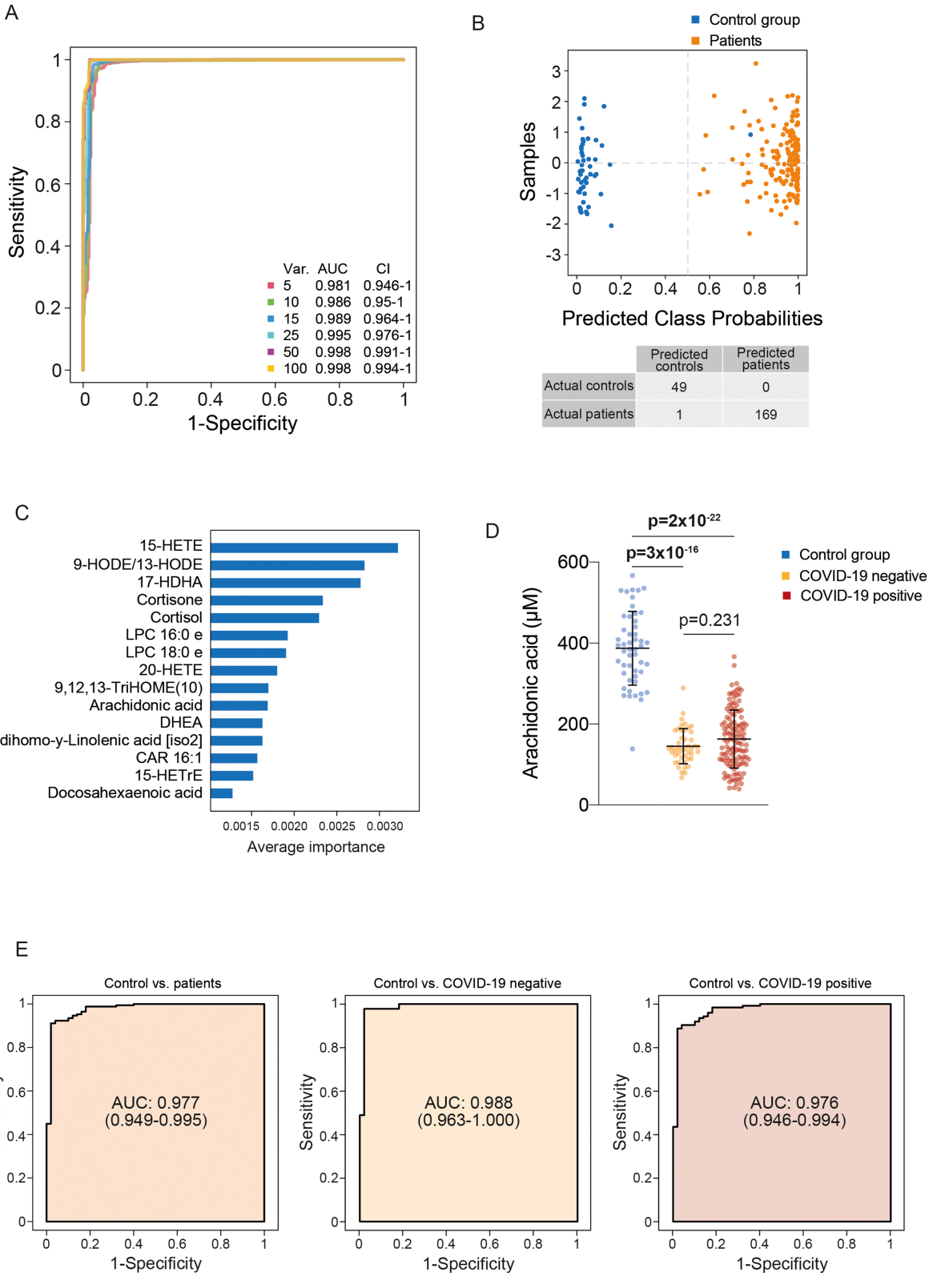
A
Sensitivity
1-Specificity
Var. AUC CI
5 0.981 0.946-1
10 0.986 0.95-1
15 0.989 0.964-1
25 0.995 0.976-1
50 0.998 0.991-1
100 0.998 0.994-1
B
Control group
Patients
Samples
Predicted Class Probabilities
Predicted controls
Predicted patients
Actual controls 49 0
Actual patients 1 169
C
15-HETE
9-HODE/13-HODE
17-HDHA
Cortisone
Cortisol
LPC 16:0 e
LPC 18:0 e
20-HETE
9,12,13-TriHOME(10)
Arachidonic acid
DHEA
dihomo-y-Linolenic acid [iso2]
CAR 16:1
15-HETrE
Docosahexaenoic acid
Average importance
D
p=2x10-22
p=3x10-16
p=0.231
Arachidonic acid (µM)
Control group
COVID-19 negative
COVID-19 positive
E
Control vs. patients
AUC: 0.977
(0.949-0.995)
Control vs. COVID-19 negative
AUC: 0.988
(0.963-1.000)
Control vs. COVID-19 positive
AUC: 0.976
(0.946-0.994)
Sensitivity
1-Specificity

Figure 3

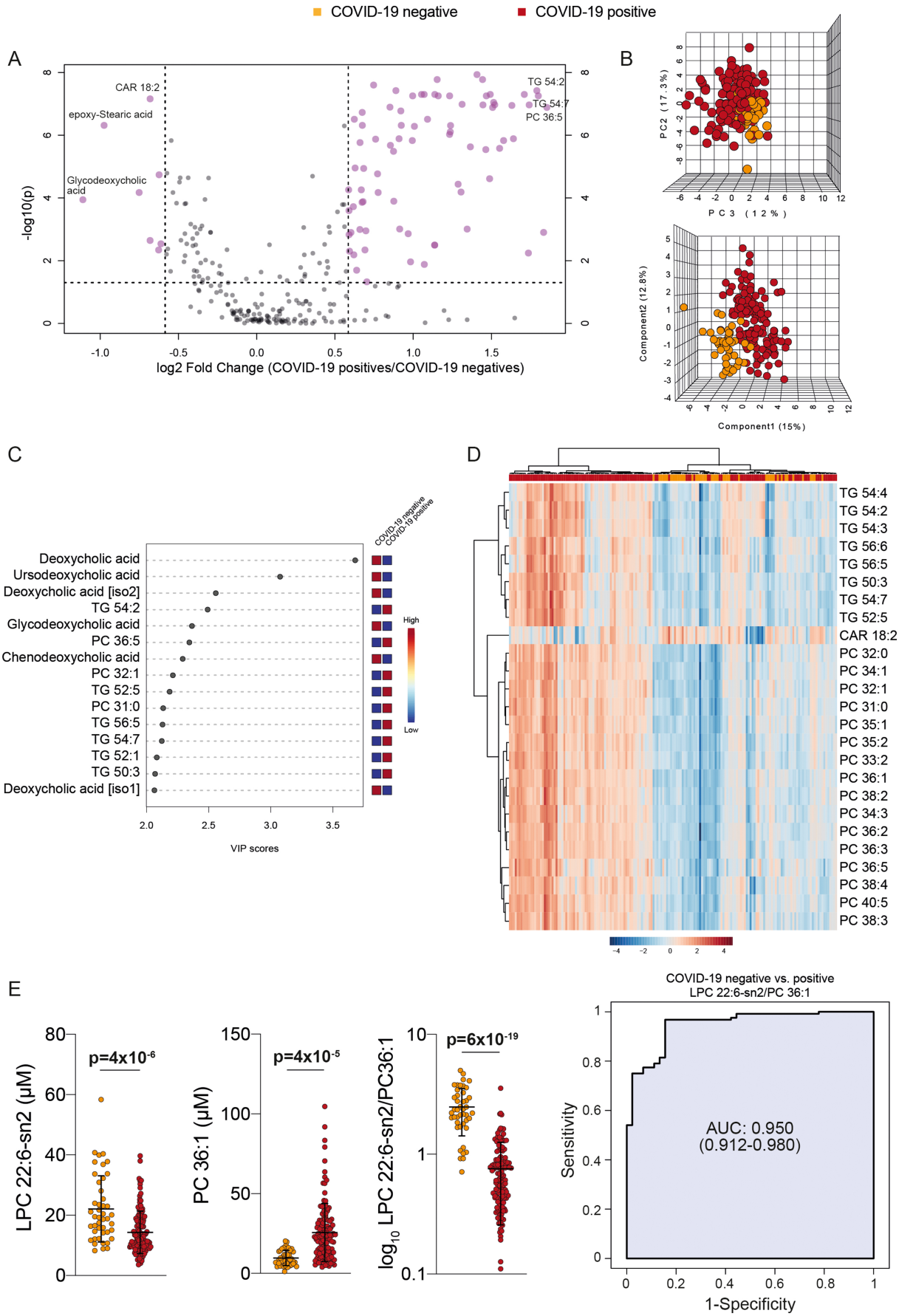
COVID-19 negative
COVID-19 positive
A
CAR 18:2
epoxy-Stearic acid
Glycodeoxycholic acid
TG 54:2
TG 54:7
PC 36:5
-log10(p)
log2 Fold Change (COVID-19 positives/COVID-19 negatives)
B
PC2 (17.3%)
PC 3 (12%)
Component2 (12.8%)
Component1 (15%)
C
Deoxycholic acid
Ursodeoxycholic acid
Deoxycholic acid [iso2]
TG 54:2
Glycodeoxycholic acid
PC 36:5
Chenodeoxycholic acid
PC 32:1
TG 52:5
PC 31:0
TG 56:5
TG 54:7
TG 52:1
TG 50:3
Deoxycholic acid [iso1]
High
Low
VIP scores
D
TG 54:4
TG 54:2
TG 54:3
TG 56:6
TG 56:5
TG 50:3
TG 54:7
TG 52:5
CAR 18:2
PC 32:0
PC 34:1
PC 32:1
PC 31:0
PC 35:1
PC 35:2
PC 33:2
PC 36:1
PC 38:2
PC 34:3
PC 36:2
PC 36:3
PC 36:5
PC 38:4
PC 40:5
PC 38:3
E
p=4x10-6
LPC 22:6-sn2 (μM)
p=4x10-5
PC 36:1 (μM)
p=6x10-19
log10 LPC 22:6-sn2/PC36:1
COVID-19 negative vs. positive
LPC 22:6-sn2/PC 36:1
AUC: 0.950
(0.912-0.980)
Sensitivity
1-Specificity

Figure 4

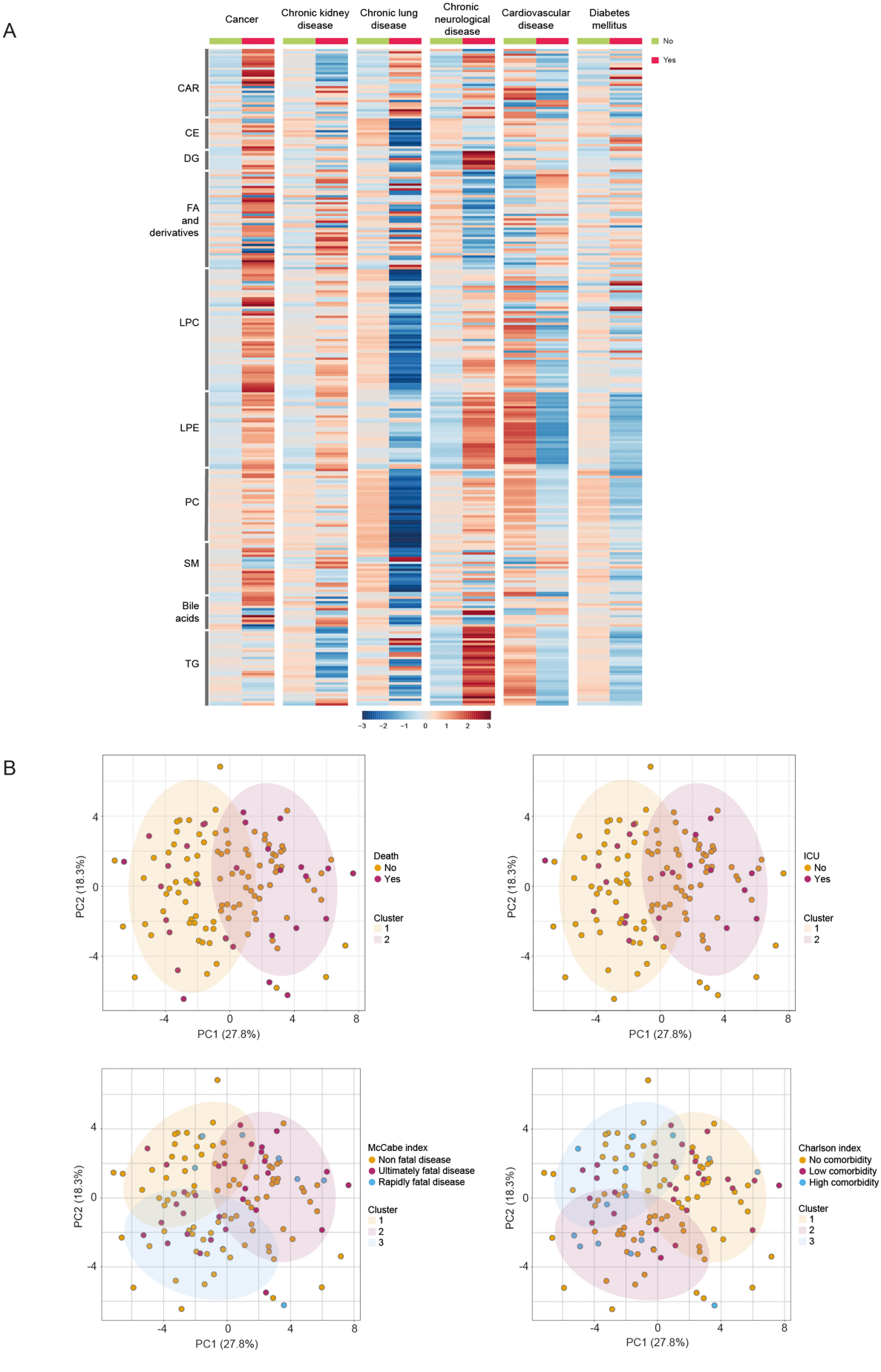
A
Cancer
Chronic kidney disease
Chronic lung disease
Chronic neurological disease
Cardiovascular disease
Diabetes mellitus
No
Yes
CAR
CE
DG
FA and derivatives
LPC
LPE
PC
SM
Bile acids
TG
−3 −2 −1 0 1 2 3
B
PC2 (18.3%)
PC1 (27.8%)
Death
No
Yes
Cluster
1
2
ICU
No
Yes
McCabe index
Non fatal disease
Ultimately fatal disease
Rapidly fatal disease
3
Charlson index
No comorbidity
Low comorbidity
High comorbidity

Figure 5